NASA TM X-53156

A STUDY OF DENSITY VARIATIONS IN FREE MOLECULAR FLOW THROUGH CYLINDRICAL DUCTS DUE TO ACCOMMODATION COEFFICIENTS

by S. J. ROBERTSON
Aero-Astrodynamics Laboratory

NASA

George C. Marshall Space Flight Center,
Huntsville, Alabama

A STUDY OF DENSITY VARIATIONS IN FREE MOLECULAR FLOW
THROUGH CYLINDRICAL DUCTS DUE TO ACCOMMODATION COEFFICIENTS

By

S. J. Robertson*

George C. Marshall Space Flight Center

Huntsville, Alabama

ABSTRACT

14934

A theoretical investigation was made of free-molecule flow through a duct of circular cross section. The molecular flux to the duct wall and exit plane was calculated along with the total flow rate through the duct. The density field was calculated at the duct exit and along the centerline for various duct wall temperatures and thermal accommodation coefficients. It was concluded that an experimental determination of the thermal accommodation coefficient can be made by measuring the effect of the duct wall temperature on the density field.

NASA - GEORGE C. MARSHALL SPACE FLIGHT CENTER

NASA - GEORGE C. MARSHALL SPACE FLIGHT CENTER

Technical Memorandum X-53156

November 2, 1964

A STUDY OF DENSITY VARIATIONS IN FREE MOLECULAR FLOW
THROUGH CYLINDRICAL DUCTS DUE TO ACCOMMODATION COEFFICIENTS

By

S. J. Robertson

THERMOENVIRONMENT BRANCH
AERODYNAMICS DIVISION
AERO-ASTRODYNAMICS LABORATORY

TABLE OF CONTENTS

LIST OF ILLUSTRATIONS

DEFINITION OF SYMBOLS

Symbol	Definition
$(F_{IW})_{x/L}$	form factor for flux from duct entrance to a point on wall at a dimensionless distance x/L from entrance
$(F_{WW})_{|(x/L)-(\ell/L)|}$ $\delta\ell$	form factor for flux from a ring element $\delta\ell$ wide of duct wall to a point on the wall at a dimensionless distance $|(x/L) - (\ell/L)|$
$(F_{IE})_{r/R}$	form factor for flux from entrance to a point r/R on exit
$(F_{WE})_{x/L, r/R}$ $\delta\ell$	form factor for flux from a ring element $\delta\ell$ wide of duct wall a dimensionless distance x/L from entrance to a point r/R on exit
L	duct length
M	molecular weight
n	number of collisions
q_o	molecular flux from reservoir to entrance plane
$(q_E/q_o)_{r/R, n}$	dimensionless molecular flux to exit plane at r/R for molecules reaching exit after n collisions
$(q_E/q_o)_{r/R}$	total dimensionless molecular flux to exit plane at r/R
$(q_W/q_o)_{x/L, n}$	dimensionless molecular flux to duct wall at x/L for molecules reaching point on wall after n collisions
$(q_W/q_o)_{x/L}$	total dimensionless molecular flux to duct wall at x/L
Q_E	total flow rate
r	radial distance
R	duct radius
$\mathcal{R}$	universal gas constant

DEFINITION OF SYMBOLS (Continued)

Symbol	Definition
T_o	reservoir gas temperature
T_s	duct wall temperature
T_n	gas temperature after n collisions
$\bar{v}$	mean molecular velocity
$\bar{v}_o$	reservoir mean molecular velocity
x	axial distance from duct entrance
α	thermal accommodation coefficient
ρ_o	reservoir number volume density of gas molecules
$(\rho/\rho_o)_{r/R,n}$	dimensionless number volume density at r/R on exit for molecules reaching exit after n collisions
$(\rho/\rho_o)_{r/R}$	total dimensionless number volume density at r/R on exit
$(\rho/\rho_o)_{x/L,n}$	dimensionless number volume density at x/L on centerline for molecules reaching exit after n collisions
$(\rho/\rho_o)_{x/L}$	total dimensionless number volume density at x/L on centerline

A STUDY OF DENSITY VARIATIONS IN FREE MOLECULAR.FLOW THROUGH CYLINDRICAL DUCTS DUE TO ACCOMMODATION COEFFICIENTS

SUMMARY

A theoretical investigation was made of free-molecule flow through a duct of circular cross section. The molecular flux to the duct wall and exit plane was calculated along with the total flow rate through the duct. The density field was calculated at the duct exit and along the centerline for various duct wall temperatures and thermal accommodation coefficients. It was concluded that an experimental determination of the thermal accommodation coefficient can be made by measuring the effect of the duct wall temperature on the density field.

I. INTRODUCTION

Recent requirements for space environment simulation facilities have resulted in increased effort toward understanding and predicting the behavior of low density gas flow. Many of these studies have been directed toward the prediction of flow rates through complicated duct systems, the development of cryopanel shapes for optimum pumping speeds in high vacuum systems, and the prediction of the properties of the flow field surrounding bodies in high velocity flight in the upper atmosphere.

Free-molecule flow rates through tubes were first investigated theoretically and experimentally by Knudsen [1]. These studies were made for flow in long capillary tubes (the tube length being much longer than its radius) for which end effects may be neglected. Clausing [2] later extended the flow rate theory to the case of short tubes and ducts. The same mathematical problem was solved independently and almost simultaneously by Hottel and Keller [3] for the case of thermal radiation through furnace openings. Hottel and Keller's results are nearly identical with Clausing's. The accuracy of Clausing's solution was verified nearly 20 years later by Demarcus and Hopper [4].

Other investigators [5, 6, 7, 8, 9, 10, 11] have studied molecular flux and flow rates for various conditions of free-molecule flow.

The calculation of density fields for free-molecule flow was made by Bird [12] for the field about moving bodies of various geometries, Touryan [13] for the flow over a circular plate, and Howard [14] and Gustafson and Kiel [15] for flow through orifices.

Sparrow and Haji-Sheikh [16] investigated, among other parameters, the density field through circular ducts for the case of perfect thermal accommodation of the molecules at the duct wall (a thermal accommodation coefficient of the duct wall material of unity).

The purpose of this study is to determine theoretically the flow rate and density field through a circular duct at various duct wall temperatures and thermal accommodation coefficients.

II. ANALYSIS AND DISCUSSION OF RESULTS

Consider the following illustrated circular duct:
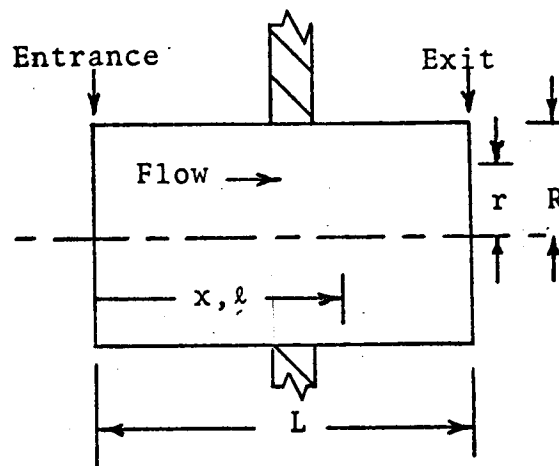
The entrance is exposed to an infinitely large reservoir of rarefied Maxwellian gases at density, ρ_o, and temperature, T_o, while the exit is exposed to a vacuum. The dimensions of the duct are small in comparison to the mean free path of the gas molecules so that the flow of molecules in the duct may be considered "free-molecular"; i.e., intermolecular collisions may be neglected in comparison to the collisions of molecules with the duct wall. Diffuse (cosine law) scattering of the molecules by the wall will be assumed. (Experiments by Knudsen [17] and others on the reflection of molecular beams from glass and polished metal surfaces indicate nearly 100 percent diffuse reflection.) Moreover, it is assumed that the system is in equilibrium and that all molecules incident on a surface are reflected without adsorption, outgassing, or surface reactions.

2

The molecular flux for molecules leaving the reservoir at the duct entrance is [21]:

$$q_o = \rho_o \; (\mathcal{R}T_o/2\pi M)^{1/2}.$$

Some of these molecules pass through the duct without any collisions. Those molecules that collide with the wall may, after one or more collisions, finally leave the duct through the exit or be scattered back into the reservoir.

With each collision, the molecule will gain or lose some of its energy, the amount of gain or loss depending on the duct wall temperature and the thermal accommodation coefficient. Although this gain or loss of energy does not influence the probability of eventual passage through the duct (and, hence, the equilibrium flow rate), it does influence the density field.

It has been shown [1, 2, 3] that it is not necessary to consider each collision in computing molecular flux and flow rates. Since each collision affects the density field, however, it was convenient to calculate the contribution to the molecular flux of each collision with its resulting contribution to the density field.

A. Molecular Flux and Flow Rates

There are two distinct methods now in use for computing molecular flux and flow rates under highly rarefied conditions. The first method, known as the Monte Carlo technique, is particularly well suited to complicated geometrical shapes. This method traces many individual particles through randomly chosen paths. A sufficient number of these random paths is traced to statistically determine the most probable distribution of particles over the geometrical shape. This method was used by Ballance, Roberts, and Tarbell [18] to study molecular fluxes for various cryoarray configurations in a high vacuum cryopumping system. It was also used by Davis [19], to calculate the flow rate through ducts of various shapes.

The second method, designated the "molecular kinetics" method by Link [20], is based on the analogy between radiant energy transfer and free-molecule kinetics [20, 21]. The procedure used in this method is to subdivide the geometry into discrete elements for which a radiation "form factor" may be calculated. This method, particularly useful for simple geometries for which published values of form factors exist, will be used in the present study.

1. Molecular Flux to Duct Wall

Based on radiation analogy principles, the molecular flux to the wall of the previously illustrated duct due to a collisionless passage from the reservoir is

$$(q_W/q_o)_{x/L,o} = (F_{IW})_{x/L},\tag{2}$$

where [22]

$$(F_{IW})_{x/L} = (1/2) \left\{ \frac{(L/R)^2(x/L)^2 + 2}{[(L/R)^2 (x/L)^2 + 4]^{1/2}} - (L/R)(x/L) \right\}.\tag{3}$$

The molecular flux on the duct wall for molecules reaching the wall after n collisions is

$$(q_W/q_o)_{x/L,n} = \int_o^1 (F_{WW})_{|(x/L) - (\ell/L)|} \; (q_W/q_o)_{\ell/L,n-1} \; d(\ell/L),\tag{4}$$

where [3]

$$(F_{WW})_{|(x/L) - (\ell/L)|} = (1/2)(L/R) \Bigg\langle 1 - $$

$$(L/R)|(x/L) - (\ell/L)| \frac{(L/R)^2 [(x/L) - (\ell/L)]^2 + 6}{\left\{ (L/R)^2 [(x/L) - (\ell/L)]^2 + 4 \right\}^{3/2}} \Bigg\rangle.\tag{5}$$

4

The total molecular flux on the duct wall is obtained by summing the fluxes for each collision as follows:

$$(q_W/q_o)_{x/L} = \sum_{n=0}^{\infty} (q_W/q_o)_{x/L,n}. \qquad (6)$$

The total molecular flux at the duct wall surface was calculated from equations (2), (4), and (6) for a duct of dimensions, $L/R = 2.0$. Equation (4) was integrated numerically by the procedure described in Appendix A. The summation in equation (6) was carried out to 20 collisions. The results are presented in Figure 1 along with the contributions of the first few collisions. It is seen that the contributions rapidly become insignificant after a few collisions. Also, the total flux distribution is remarkably linear. Hottel [3] made the same observation in his radiation analysis and suggested that a simple solution of the problem could be made by assuming a linear total wall flux distribution and then solving for the exit flux.

2. Molecular Flux at Exit Plane

The exit molecular flux at radial position r/R for a collisionless passage from the reservoir through the duct is

$$(q_E/q_o)_{r/R,o} = (F_{IE})_{r/R}, \qquad (7)$$

where [22]

$$(F_{IE})_{r/R} = (1/2) \left\langle 1 - \frac{(L/R)^2 + (r/R)^2 - 1}{\left\{ [(L/R)^2 + (r/R)^2 + 1]^2 - 4(r/R)^2 \right\}^{1/2}} \right\rangle. \qquad (8)$$

The molecular flux for molecules reaching the exit after n collisions is

$$(q_E/q_o)_{r/R,n} = \int_o^1 (F_{WE})_{x/L,r/R} \, (q_W/q_o)_{x/L,n-1} \, d(x/L), \qquad (9)$$

5

where

$$(F_{WE})_{x/L, r/R}$$

$$= 2(L/R)^2(1 - x/L) \frac{(L/R)^2(1 - x/L)^2 - (r/R)^2 + 1}{\left\{[(L/R)^2(1 - x/L)^2 + (r/R)^2 + 1]^2 - 4(r/R)^2\right\}^{3/2}} \cdot$$

(10)

Equation (10) is derived in Appendix B.

As in the case of the flux to the duct wall, the total flux to a point on the exit is obtained by summing the contributions for each collision:

$$(q_E/q_o)_{r/R} = \sum_{n=0}^{\infty} (q_E/q_o)_{r/R, n} \cdot$$

(11)

The contribution to the center exit flux for each collision is presented in Figure 2 as a function of collision number for a duct with dimensions, $L/R = 2.0$. (Again, the equations were integrated numerically by the procedure of Appendix A, and the summation was carried to 20 collisions). As shown previously for the wall flux, the contribution rapidly becomes insignificant with increasing collision number.

The total flux distribution over the exit is shown in Figure 3 along with the contributions of the first few collisions. An interesting characteristic of the distribution curves is their boundary-layer-like decrease in magnitude at the edge of the duct. This curvature is displayed by all contributions involving one or more collisions.

3. Total Flow Rate

The total flow rate through the duct is obtained by integrating the total molecular flux distribution over the exit:

$$Q_E/q_o = \int (q_E/q_o)_{r/R} \, dA = 2\pi R^2 \int_0^1 (q_E/q_o)_{r/R} \, (r/R) \, d(r/R).$$

(12)

6

The flow rate through ducts of several L/R ratios was calculated numerically from equation (12) by the procedure of Appendix C and is presented in Figure 4 compared with Clausing's [2] calculations. For an L/R ratio of 2.0, there is a difference of 0.1 percent for the present calculations when compared with Clausing's.

B. Density Fields

The number volume density ρ of molecules at a point due to the flux from an element of area dA at a distance d from the point is determined by [12]

$$d\rho = q \cos \theta \, dA/\bar{v}\Pi d^2 = (q/\bar{v})(d\omega/\Pi), \tag{13}$$

where $d\omega = \cos \theta \, dA/d^2$, q is the flux from the surface element dA, θ is the angle between the normal to dA and the line d, and $\bar{v}$ is the mean velocity of the molecules.

The reservoir flux (the flux from the reservoir to the duct entrance) q_o, can be expressed in terms of the far upstream reservoir density and mean molecular velocity as follows [21]:

$$q_o = (1/4) \, \rho_o \bar{v}_o. \tag{14}$$

Combining equations (13) and (14) yields

$$d\rho/\rho_o = (1/4) \, [(q/q_o)/(\bar{v}/\bar{v}_o)] \, (d\omega/\Pi). \tag{15}$$

For the density due to the flux directly from the reservoir, the flux and mean velocity ratios become unity and the density is found from

$$(\rho/\rho_o)_{r/R,o} = (1/4) \int d\omega/\Pi, \tag{16}$$

where the integration is over the solid angle enclosed by the duct entrance.

1. Density at Exit Plane

The center exit density due to a collisionless passage from the reservoir is found from equation (16) to be (Appendix D)

$$(\rho/\rho_o)_{o,o} = (1/2) \left\{ 1 - \frac{(L/R)}{[(L/R)^2 + 1]^{1/2}} \right\}. \tag{17}$$

For positions on the exit other than center, equation (16) is integrated numerically by the procedure described in Appendix D.

The equation for the density at r/R for molecules reaching the exit after n collisions, obtained from equation (15), is

$$(\rho/\rho_o)_{r/R,n} = \frac{1}{4(T_n/T_o)^{1/2}} \int (q_w/q_o)_{x/L,n-1} \, (d\omega/\Pi), \tag{18}$$

where (Appendix E)

$$T_n/T_o = (1 - \alpha)^n + \alpha(T_s/T_o) \sum_{i=o}^{n-1} (1 - \alpha)^i \tag{19}$$

and the integration is performed numerically over the solid angle enclosed by the duct wall by the procedure described in Appendix D. The mean velocity ratio is equal to the square root of the temperature ratio because of the assumption of a Maxwellian velocity distribution at all times (12).

The contribution to the center exit density is presented in Figures 5 and 6 as a function of collision number for a duct of dimensions, L/R = 2.0, and various duct temperatures and thermal accommodation coefficients. As with the molecular flux, the contributions rapidly become insignificant with increasing collision number.

The total density at a point on the exit is found by summing the contributions for each collision:

8

$$\left(\rho/\rho_0\right)_{r/R} = \sum_{n=o}^{\infty} \left(\rho/\rho_0\right)_{r/R,n}. \qquad (20)$$

As with the total flux calculations, the summation was carried out to 20 collisions for these results.

The total exit density distribution is shown in Figure 7 along with the contributions of the first few collisions for a duct of dimensions L/R = 2.0 with a duct to reservoir temperature ratio T_s/T_o of unity. The variation of the total exit density distribution with duct temperature is shown in Figure 8 for a duct of the same dimensions with a thermal accommodation coefficient of unity. As with the flux distribution, there is a sharp boundary-layer-like decrease in magnitude at the edge. It is also observed that the exit density decreases with increasing duct temperature.

Figure 9 shows the variation of exit density distribution with thermal accommodation coefficient for two duct temperatures. For a duct to reservoir temperature ratio, T_s/T_o, greater than unity, the density ratio ρ/ρ_0 increases with decreasing thermal accommodation coefficient α, while for T_s/T_o less than unity, ρ/ρ_0 decreases with decreasing α. In both cases ρ/ρ_0 approaches the condition for T_s/T_o equal to unity as α approaches zero. Equation (19) shows that T_s/T_o equal to unity with any α yields the same results as T_s/T_o not equal to unity with an α equal to zero.

In Figures 10 and 11 is shown the variation of the center exit density with duct temperature and thermal accommodation coefficient for ducts of dimensions L/R = 2.0 and L/R = 4.0. Comparing the two figures shows that the density has decreased considerably by increasing L/R. Notice that the curves intersect at $T_s/T_o = 1.0$ and spread as T_s/T_o approaches zero or infinity. The amount of density variation shown in these figures indicates the feasibility of an experimental determination of the thermal accommodation coefficient by measuring the effect of the duct wall temperature on the density field.

2. Density on Centerline

The centerline density distribution is found by integrating equations (15) and (16) from a point on the centerline. The resulting equations are

$$\left(\rho/\rho_0\right)_{x/L,o} = (1/2) \left\{ 1 - \frac{(L/R)\,(x/L)}{[(L/R)^2(x/L)^2 + 1]^{1/2}} \right\} \qquad (21)$$

9

for zero collisions, and

$$(\rho/\rho_o)_{x/L,n} = \frac{1}{4(T_n/T_o)^{1/2}} \int (q_w/q_o)_{\ell/L,n-1} \; (d\omega/\Pi) \tag{22}$$

for n collisions. Equation (22) is integrated numerically over the solid angle enclosed by the duct wall in a manner similar to the integration of equation (18). The derivation of equation (21) and the procedure for integrating equation (22) is described in Appendix D. The total density is obtained by summing the contributions for each collision.

The total centerline density distribution is presented in Figure 12 along with the contributions of the first few collisions for a duct of dimensions L/R = 2.0 and a duct to reservoir temperature ratio T_s/T_o of unity. The variation of the centerline density distribution with duct temperature is shown in Figure 13 for a duct with the same dimensions as in Figure 12 and with a thermal accommodation coefficient of unity. It is seen that the total density ratio ρ/ρ_o approaches unity for upstream of the duct and zero far downstream. The variation in density with duct temperature appears to be most pronounced in the second quarter segment downstream of the duct entrance.

The variation of centerline density distribution with thermal accommodation coefficient is shown in Figure 14 for two duct temperatures. The variation here follows the same pattern as in Figure 9.

C. Accuracy of Results

It was mentioned in the discussion of flow rates that for an L/R ratio of 2.0 the present calculations of flow rates are within 0.1 percent of the results of Clausing [2]. Demarcus [4] showed that Clausing's flow rate calculation for a duct of those dimensions are correct to within 0.12 percent. Since the present calculations of density are computed essentially in the same manner as the present calculations of molecular flux and flow rates, it is inferred that the density results are correct to within at most one or two percent.

D. Computer Program

The calculations described herein were performed on an IBM 7090 computer. The computer program was written in Fortran IV language and is presented in Appendix F.

10

III. POSSIBLE EXPERIMENTAL VERIFICATION

Most of the available publications dealing with density measurements in rarefied gas flow describe techniques using scattering and attenuation of various beams such as electron beams [23, 24] and gamma radiation [25]. It is recommended that the electron beam scattering technique described in References 23 and 24 be investigated as the most promising approach to experimental verification of the results in this report.

IV. CONCLUSIONS

1. Nearly all of the molecules which pass through a duct of dimensions L/R = 2.0 under conditions of free molecule flow have fewer than 10 internal collisions during passage through the duct.

2. The molecular flux to the duct wall is a nearly linear function of axial distance for a duct of dimensions L/R = 2.0.

3. The molecular flux and volume density are nearly uniformly distributed over the duct exit with the exception of a sharp boundary-layer-like decrease in magnitude at the edge.

4. For a duct of dimensions L/R = 2.0 with a thermal accommodation coefficient of unity, an increase by a factor of two in the duct temperature from the ambient gas temperature results in a decrease in exit density of approximately 30 percent.

5. An experimental determination of the thermal accommodation coefficient by measuring the effect of the duct wall temperature on the density field appears feasible.

6. Reference 27 obtained exit flux distributions for circular ducts, but the method used was believed to be unreliable for positions on the exit plane near the wall. The curves, therefore, were extended through this region so that the "boundary layer" effects noted in this study were not shown.

APPENDIX A

PROCEDURE FOR NUMERICAL INTEGRATION OF FLUX EQUATIONS

The numerical integrations of equations (4) and (9) were accomplished by dividing the duct into 50 identical circular elements as illustrated below:

Entrance   Exit
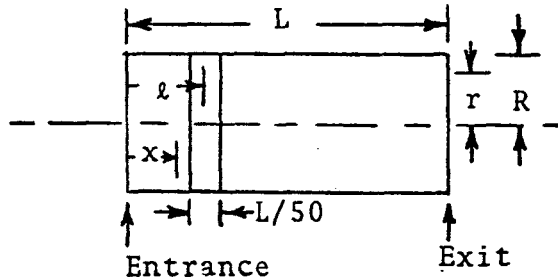
The average value of (q_W/q_o) and F_{WW} over a ring element are taken to be those calculated at the circle halving the element. Equation (4) then becomes

$$(q_W/q_o)_{x/L,n} = (1/50) \sum_{i=1}^{50} \left\{ (F_{WW}) \Big| (x/L)-(i-1/2)/50 \Big| \right\} (q_W/q_o)_{(i-1/2)/50,n-1}.$$
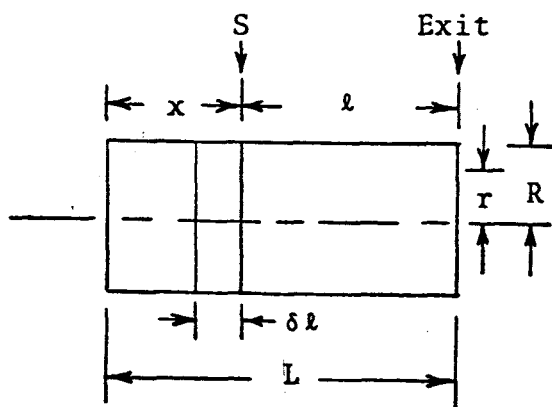
(A-1)

Equation (9) becomes

$$(q_E/q_o)_{r/R,n} = (1/50) \sum_{i=1}^{50} \left\{ (F_{WE})_{(i-1/2)/50,r/R} \right\} (q_W/q_o)_{(i-1/2)/50,n-1}.$$

(A-2)

13

APPENDIX B

DERIVATION OF WALL TO EXIT FORM FACTOR

The form factor given by equation (10) is derived by the method of Reference 3 using the following illustration.

The molecular flux at r on the exit due to collisionless traversing of molecules from a disc S enclosed by a cylinder at a distance ℓ from the exit is

$$q_E = F(\ell)\dot{q},$$

(B-1)

where q is the flux across the disc S.

The flux from a disc at $\ell + \delta\ell$ from the exit is

$$q_E + \delta q_E = F(\ell)q + F'(\ell)\,\delta\ell q.$$

(B-2)

The quantity $\delta q_E = F'(\ell)\,\delta\ell$ is actually negative due to decreasing $F(\ell)$ with increasing ℓ and may be considered due to the flux q from the wall strip enclosed by $\delta\ell$.

Therefore, the form factor for flux from a wall element $\delta\ell$ wide is $-F'(\ell)\delta\ell$.

The form factor, F, for flux from the disc S in the preceding illustration is [22]

$$F = (1/2)\left\langle 1 - \frac{(r/R)^2 + (L/R)^2\,(\ell/L)^2 - 1}{\left\{[r/R]^2 + (L/R)^2\,(\ell/L)^2 + 1]^2 - 4(r/R)^2\right\}^{1/2}}\right\rangle.$$

(B-3)

The form factor given by equation (10) is obtained from equation (B-3) by

$$(F_{WE})_{\ell/L,\,r/R} = -F'(\ell)$$

$$= 2(L/R)^2(\ell/L)\,\frac{(L/R)^2(\ell/L)^2 - (r/R)^2 + 1}{\left\{[L/R]^2(\ell/L)^2 + (r/R)^2 + 1]^2 - 4(r/R)^2\right\}^{3/2}}$$

(B-4)

or

$$(F_{WE})_{x/L,\,r/R}$$

$$= 2(L/R)^2(1 - x/L)\,\frac{(L/R)^2\,(1 - x/L)^2 - (r/R)^2 + 1}{\left\{[(L/R)^2(1 - x/L)^2 + (r/R)^2 + 1]^2 - 4(r/R)^2\right\}^{3/2}}.$$

(B-5)

16

APPENDIX C

INTEGRATION PROCEDURE FOR TOTAL FLOW RATE

The numerical procedure for integrating equation (12) is similar to the procedure described in Appendix A. In this case, however, the trapezoidal rule was used as follows:

$$Q_E / \pi R^2 q_o = 2 \int_0^1 (q_E/q_o)_{r/R} \, (r/R) \, d(r/R)$$

$$= (1/1250) \sum_{i=1}^{49} i(q_E/q_o)_{i/50} + (1/50)(q_E/q_o)_{1.0}, \qquad (C-1)$$

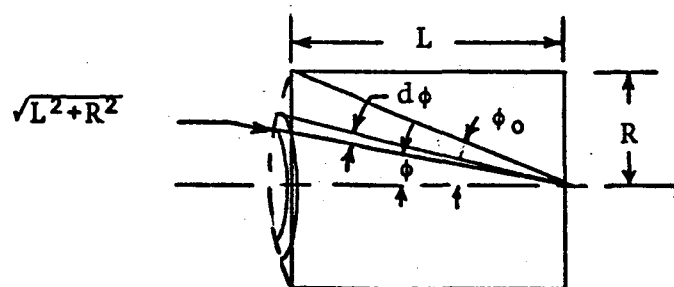where i is an integer from one to 49 and the radius R is divided into 50 equal elements R/50.

APPENDIX D

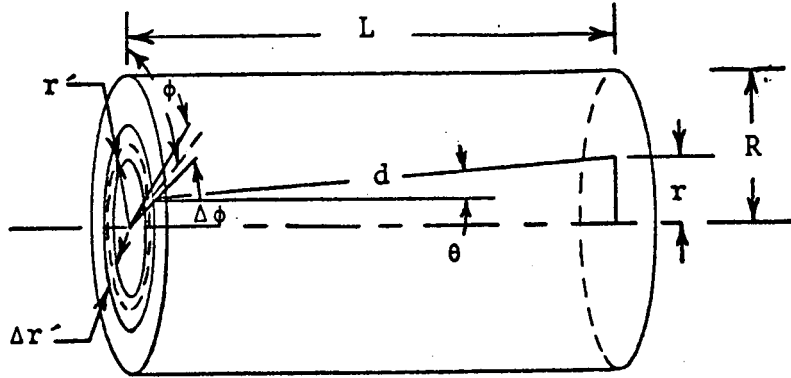DERIVATION OF DENSITY EQUATIONS

A. Exit Density

1. Zero Collisions

The center exit density for zero collisions is obtained by integrating equation (16) over the solid angle enclosed by the entrance as illustrated.

$$(\rho/\rho_0)_{0,0'} = (1/4) \int d\omega/\Pi$$

$$= (1/2) \int_0^{\phi_0} \sin\phi \, d\phi \qquad\qquad (D-1)$$

$$= (1/2) \left\{ 1 - \frac{(L/R)}{[(L/R)^2 + 1]^{1/2}} \right\}.$$

For positions on the exit other than center a numerical integration is performed as illustrated.

The element of solid angle $\Delta\omega$ enclosed by the element of area defined by $\Delta\phi$ and $\Delta r'$ is (equation (13)):

$$\Delta\omega = \lim_{\substack{\Delta\phi \to 0 \\ \Delta r \to 0}} r'\Delta\phi\,\Delta r'\,\cos\theta/d^2,$$

(D-2)

where r' and ϕ are taken at the midpoint of the element. Now

$$\cos\theta = L/d$$

(D-3)

and

$$d = (L^2 + r^2 + r'^2 - 2rr'\cos\phi)^{1/2}.$$

(D-4)

We will choose $\Delta r' = R/20$ and $\Delta\phi = \Pi/20$. Equation (D-2) then becomes

$$\Delta\omega = \frac{(\Pi/8000)\,(L/R)\,(i - 1/2)}{\left\{(L/R)^2 + (r/R)^2 + \frac{(i - 1/2)^2}{400} - \frac{(i - 1/2)}{10}\,(r/R)\,\cos\frac{[(j - 1/2)\Pi]}{20}\right\}^{3/2}},$$

(D-5)

where i and j are integers from one to twenty.

20

The integral of equation (16) over the solid angle enclosed by the entrance would be twice the summation of equation (D-5) for i and j from one to twenty:
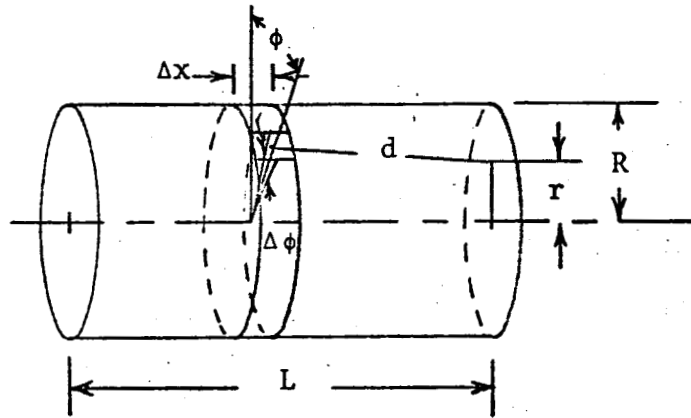
$$(\rho/\rho_0)_{r/R,o} = [(L/R)/16,000]$$

$$\sum_{j=1}^{20} \sum_{i=1}^{20} \frac{(i - 1/2)}{\left\{(L/R)^2 + (r/R)^2 + \frac{(i - 1/2)^2}{400} - \frac{(i - 1/2)}{10} (r/R) \cos \frac{[(j - 1/2)\text{II}]}{20}\right\}^{3/2}} \cdot$$

(D-6)

2. n Collisions

The exit density for n collisions is obtained by integrating equation (18) in a manner similar to the above described integration of equation (16):

The element of solid angle $\Delta\omega$ enclosed by the element of area defined by $\Delta\phi$ and Δx is (equation (13))

$$\Delta\omega = \lim_{\substack{\Delta\phi \to 0 \\ \Delta x \to 0}} R\Delta\phi\Delta x(R - r \cos \phi)/d^3$$

21

We choose $\Delta x = L/50$ and $\Delta \phi = \Pi/20$ so that equation (D-7) becomes

$$\Delta \omega = \frac{\Pi[(L/R)/1000] \left\{ 1 - (r/R) \cos [(j - 1/2)\Pi/20] \right\}}{\left\{ 1 + (L/R)^2 \left[1 - \frac{(i - 1/2)}{50} \right]^2 + (r/R)^2 - 2(r/R) \cos \left[\frac{(j - 1/2)\Pi}{20} \right] \right\}^{3/2}} ,$$

(D-8)

where i is an integer from one to fifty and j is an integer from one to twenty. The integral of equation (18) over the solid angle enclosed by the duct wall would then become

$$(\rho/\rho_o)_{r/R,n} = \frac{(L/R)}{2000 \, (T_n/T_o)^{1/2}} \sum_{i=1}^{50} (q_w/q_o)_{(i-1/2)/50,n-1}$$

$$\cdot \sum_{j=1}^{20} \frac{1 - (r/R) \cos [(j - 1/2)\Pi/20]}{\left\{ 1 + (L/R)^2 \left[1 - \frac{(i - 1/2)}{50} \right]^2 + (r/R)^2 - 2(r/R) \cos \left[\frac{(j - 1/2)\Pi}{20} \right] \right\}^{3/2}} \cdot$$

(D-9)

B. Centerline Density
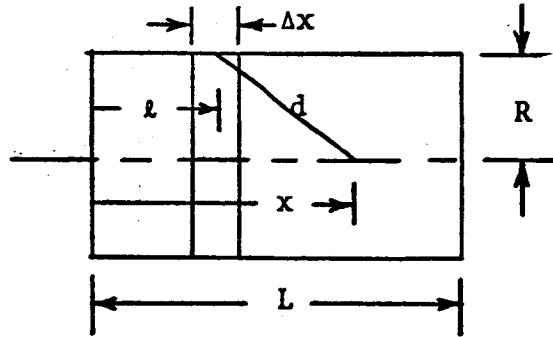
1. Zero Collisions

The derivation of the centerline density equation for zero collisions is very similar to that derived for the center exit:
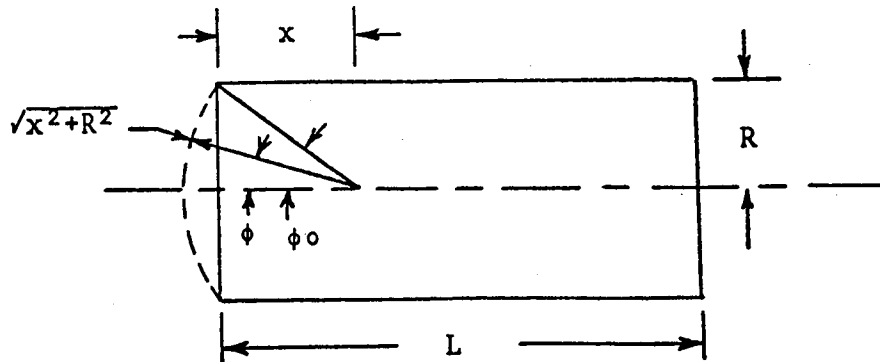
$$(\rho/\rho_0)_{x/L,0} = (1/2) \int_0^{\phi_0} \sin\phi \, d\phi = (1/2) \left\{ 1 - \frac{(L/R)(x/L)}{[(L/R)^2(x/L)^2 + 1]^{1/2}} \right\} .$$

(D-10)

2. n Collisions

The centerline density for n collisions is obtained by integrating equation (22) over the solid angle enclosed by the duct wall:

The element of solid angle $\triangle x$ enclosed by the ring element of duct wall $\triangle x$ is

$$\triangle\omega = \lim_{\triangle x \to 0} 2\pi R^2 \, \triangle x/d^3 .$$

(D-11)

We will choose $\triangle x = L/50$ so that equation (D-11) becomes

$$\triangle\omega = \frac{(\pi/25)(L/R)}{\left\{ 1 + (L/R)^2 \left[(x/L) - \frac{(i - 1/2)}{50} \right]^2 \right\}^{3/2}} ,$$

(D-12)

where i is an integer from one to 50.

23

The average value of

$$(q_W/q_o)_{x/L,n-1}$$

over a ring element was taken to be the value calculated at the circle halving the element. The integral in equation (22) then becomes

$$(\rho/\rho_o)_{x/L,n} = \frac{(L/R)}{100(T_n/T_o)^{1/2}} \sum_{i=1}^{50} \frac{(q_W/q_o)_{(i-1/2)/50,\,n-1}}{\left\{1 + (L/R)^2\left[(x/L) - \frac{(i - 1/2)}{50}\right]^2\right\}^{3/2}} .$$

(D-13)

24

APPENDIX E

DERIVATION OF GAS TEMPERATURE AFTER n COLLISIONS

The thermal accommodation coefficient α may be defined by [26]:

$$\alpha = (T_1 - T_0)/(T_s - T_0), \tag{E-1}$$

where T_1 is the energy (temperature) of the gas leaving the surface after one collision, T_s is the surface temperature, and T_0 is the gas temperature prior to the first collision. Rearranging equation (E-1) yields the expression for the gas temperature after one collision:

$$T_1/T_0 = (1 - \alpha) + \alpha(T_s/T_0). \tag{E-2}$$

Extending this equation to the nth collision yields

$$T_n/T_0 = (1 - \alpha)^n + \alpha \sum_{i=0}^{n-1} (1 - \alpha)^i T_s/T_0. \tag{E-3}$$

APPENDIX F

COMPUTER PROGRAM

The computer program used in obtaining the results in this report is given on the following three pages written in Fortran IV language.

```
$JOB                  3S/P ARMSTRONG          ,346821,00,12,1900,
$EXECUTE              IBJOB
$IBJOB AMSTNG  LOGIC,MAP,FILES
$IBFTC MOLFLO  LIST,REF,M94,XR7,DECK
       DIMENSION SUMJ(50,51)
       DIMENSION  T(51),QE(51,51),DEN(51,51),XDEN(50,51),QW(50,51)
       DIMENSION  FWF(50,51),FWW(50,50),RQF(51),RDEN(51),RXDEN(50)
       DIMENSION  RQW(50),SQW(51)
6742   CONTINUE
       CALL MAVRIK(ERR,5HTSOTO,TSOTO,5HALPHA,ALPHA,4HMAXN,MAXN,
     1  4HXLOR,XLOR)
       IF(ERR.NE.0.) CALL DUMP
       PI=3.1415926
       N=1
       WRITE(6,9876)
9876   FORMAT(1H1,32HFREE MOLECULE FLOW THROUGH DUCTS//)
       WRITE(6,4923)TSOTO,ALPHA,XLOR
4923   FORMAT(1H ,6HTS/TO=1PE15.7,1X,6HALPHA=1PE15.7,1X,4HL/R=1PE15.7//)
       T(N)=1.
       ROR=0.
       DO 35 K=1,51
       QE(K,N)=.5*(1.-(XLOR**2+ROR**2-1.)/SQRT((XLOR**2+ROR**2+1.)**2-
     2  4.*ROR**2))
       IF(K.NE.1) GO TO 58
       DEN(K,N)=.5*(1.-XLOR/SQRT(XLOR**2+1.))
       GO TO 59
58     DEN(K,N)=0.
       DO 4 J=1,20
       DO 4 I=1,20
       XI=I
       XJ=J
       DEN(K,N)=DEN(K,N)+(XI-.5)/(XLOR**2+ROR**2+(XI-.5)**2/400.-(XI-.5)
     2  *ROR/10.*COS((XJ-.5)*PI/20.))**(3./2.)
4      CONTINUE
       DEN(K,N)=DEN(K,N)*XLOR/16000.
59     CONTINUE
       ROR=ROR+.02
35     CONTINUE
       XOL=0.01
       DO 36 L=1,50
       QW(L,N)=.5*(((XLOR**2*XOL**2+2.)/SQRT(XLOR**2*XOL**2+4.))-
     2  XLOR*XOL)
       XOL=XOL+.02
36     CONTINUE
       XOL=-1.
       DO 876  L=1,31
       XDEN(L,N)=.5*(1.-XLOR*XOL/SQRT(XLOR**2*XOL**2+1.))
       XOL=XOL+.1
876    CONTINUE
       XOL=.01
       DO 9 L=1,50
       ROR=0.
       DO 10 K=1,51
       SUMJ(L,K)=0.
       DO 361 J=1,20
       XJ=J
       SUMJ(L,K)=SUMJ(L,K)+(1.-ROR*COS((XJ-.5)/20.*PI))/(1.+XLOR**2*
     X  (1.-XOL)**2+
     2  ROR**2-2.*ROR*COS((XJ-.5)/20.*PI))**(3./2.)
361    CONTINUE
```

28

```
      FWE(L,K)=2.*XLOR**2*(1.-XOL)*(XLOR**2*(1.-XOL)**2-ROR**2+1.)/
     2  ((XLOR**2*(1.-XOL)**2+ROR**2+1.)**2-4.*ROR**2)**(3./2.)
      ROR=ROR+.02
10    CONTINUE
      XLOL=.01
      DO 11 M=1,50
      FWW(L,M)=1.-XLOR*ABS(XOL-XLOL)*(XLOR**2*(XOL-XLOL)**2+6.)/
     2  (XLOR**2*(XOL-XLOL)**2+4.)**(3./2.)
      XLOL=XLOL+.02
11    CONTINUE
      XOL=XOL+.02
9     CONTINUE
      DO 38 N=1,MAXN
      IF(N.EQ.1) GO TO 720
      SUMTS=0.
      NN=N-1
      IF(ALPHA.EQ.1.) GO TO 100
      DO 1 II=1,NN
      I=II-1
      SUMTS=SUMTS+(1.-ALPHA)**I*TSOTO
1     CONTINUE
      T(N)=(1.-ALPHA)**NN+SUMTS*ALPHA
100   IF(ALPHA.EQ.1.)T(N)=TSOTO
      ROR=0.
      DO 962 K=1,51
      DEN(K,N)=0.
      QE(K,N)=0.
      XOL=0.01
      DO 965 L=1,50
      QE(K,N)=QE(K,N)+FWE(L,K)*QW(L,NN)
      DEN(K,N)=DEN(K,N)+QW(L,NN)*SUMJ(L,K)
      XOL=XOL+.02
965   CONTINUE
      QE(K,N)=QE(K,N)/50.
      DEN(K,N)=DEN(K,N)*XLOR/(2000.*SQRT(T(N)))
      ROR=ROR+.02
962   CONTINUE
      DO  903  L=1,50
      QW(L,N)=0.
      DO 963 M=1,50
      QW(L,N)=QW(L,N)+FWW(L,M)*QW(M,NN)
963   CONTINUE
      QW(L,N)=QW(L,N)*XLOR/100.
903   CONTINUE
      XOL=-1.
      DO 902  L=1,31
      XDEN(L,N)=0.
      DO  901 M=1,50
      XM=M
      XDEN(L,N)=XDEN(L,N)+QW(M,NN)/(1.+XLOR**2*(XOL-(XM-.5)/50.)**2)
     2  **(3./2.)
901   CONTINUE
      XDEN(L,N)=XDEN(L,N)*XLOR/(100.*SQRT(T(N)))
      XOL=XOL+.1
902   CONTINUE
720   CONTINUE
      NN=N-1
      WRITE(6,596)  NN,(QE(K,N),K=1,51),(DEN(K,N),K=1,51),(XDEN(L,N),
     1 L=1,31),(QW(L,N),L=1,50)
596   FORMAT(1H0,26X,I5,10HCOLLISIONS///X,9HQE VALUES,5X,6(2X,1PE15.7)/
```

```
     1 /7(15X,6(2X,1PE15.7)//)15X,3(2X,1PE15.7)//1X,10HDEN VALUES,4X,
     2 6(2X,1PE15.7)//7(15X,6(2X,1PE15.7)//),15X,3(2X,1PE15.7)//1X,
     3 14HC.L.DEN VALUES,6(2X,1PE15.7)//4(15X,6(2X,1PE15.7)//),15X,
     4 1(2X,1PE15.7)//,1X,8HQW VALUES,5X,6(2X,1PE15.7)//7(15X,
     5 6(2X,1PE15.7)//)15X,2(2X,1PE15.7)//)
  38    CONTINUE
        DO  12 K=1,51
        RQE(K)=0.
        RDEN(K)=0.
        DO 12 N=1,MAXN
        RQE(K)=RQE(K)+QE(K,N)
        RDEN(K)=RDEN(K)+DEN(K,N)
  12    CONTINUE
        WRITE(6,592) (RQE(K),K=1,51),(RDEN(K),K=1,51)
  592   FORMAT(1H0,29HTOTAL EXIT FLUX SUM QE VALUES//8(15X,6(2X,1PE15.7)
     1 //)15X,3(2X,1PE15.7)//1X,13HTOTAL DENSITY//8(15X,6(2X,
     2 1PE15.7)//)15X,3(2X,1PE15.7)//)
        DO  69  L=1,50
        RQW(L)=0.
        DO  69 N=1,MAXN
        RQW(L)=RQW(L)+QW(L,N)
  69    CONTINUE
        DO 880  L=1,31
        RXDEN(L)=0.
        DO 880   N=1,MAXN
        RXDEN(L)=RXDEN(L)+XDEN(L,N)
  880   CONTINUE
        WRITE(6,593)(RQW(L),L=1,50),(RXDEN(L),L=1,31)
  593   FORMAT(1H0,29HTOTAL WALL FLUX SUM QW VALUES//8(15X,6(2X,
     1 1PE15.7)//)15X,2(2X,1PE15.7)//1H0,25HTOTAL CENTER LINE DENSITY//
     2 5(15X,6(2X,1PE15.7)//)15X,1(2X,1PE15.7)//)
        QEINT=0.
        DO 964 K=2,50
        XK=K-1
        QEINT=QEINT+RQE(K)*XK
  964   CONTINUE
        QEINT=QEINT/1250.+RQE(51)/50.
        WRITE(6,765) QEINT
  765   FORMAT(1H0,16HTOTAL FLOW RATE=1PE15.7/)
        GO TO 6742
        STOP
        END
 $DATA
  ALPHA=1.,TSOTO=.5,XLOR=4.0,MAXN=41,/
```
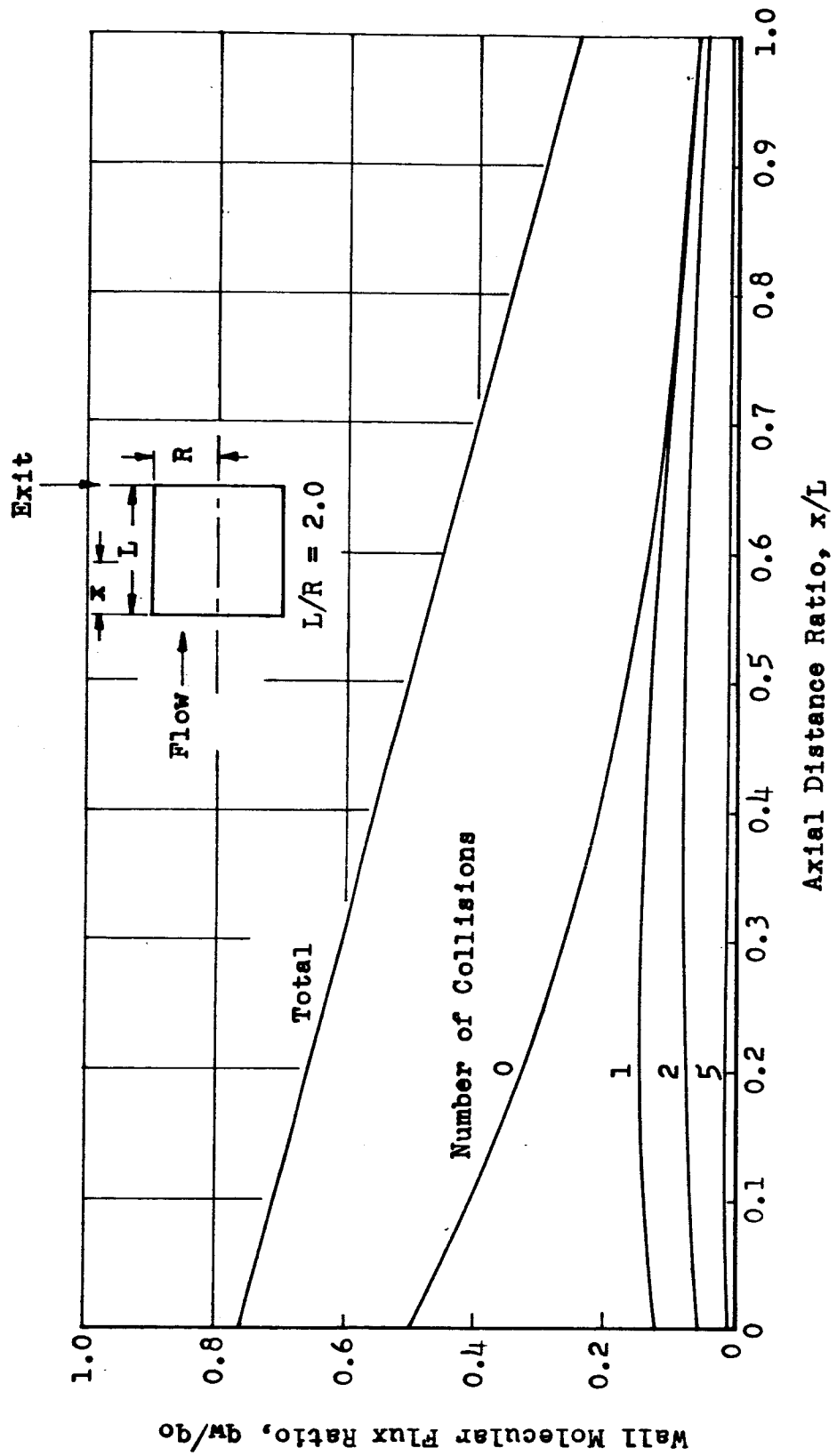
30

FIGURE 1. WALL MOLECULAR FLUX AS A FUNCTION OF
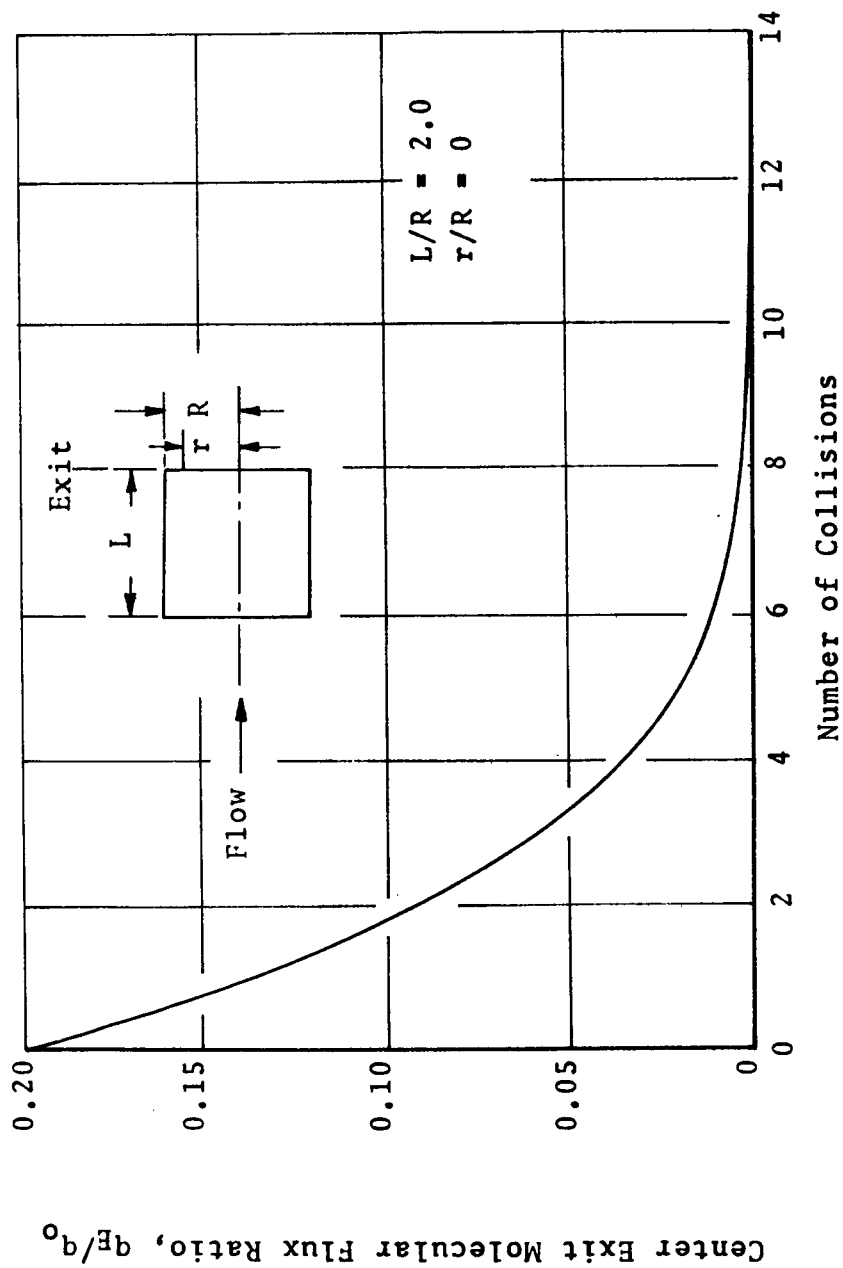NUMBER OF COLLISIONS AND POSITION

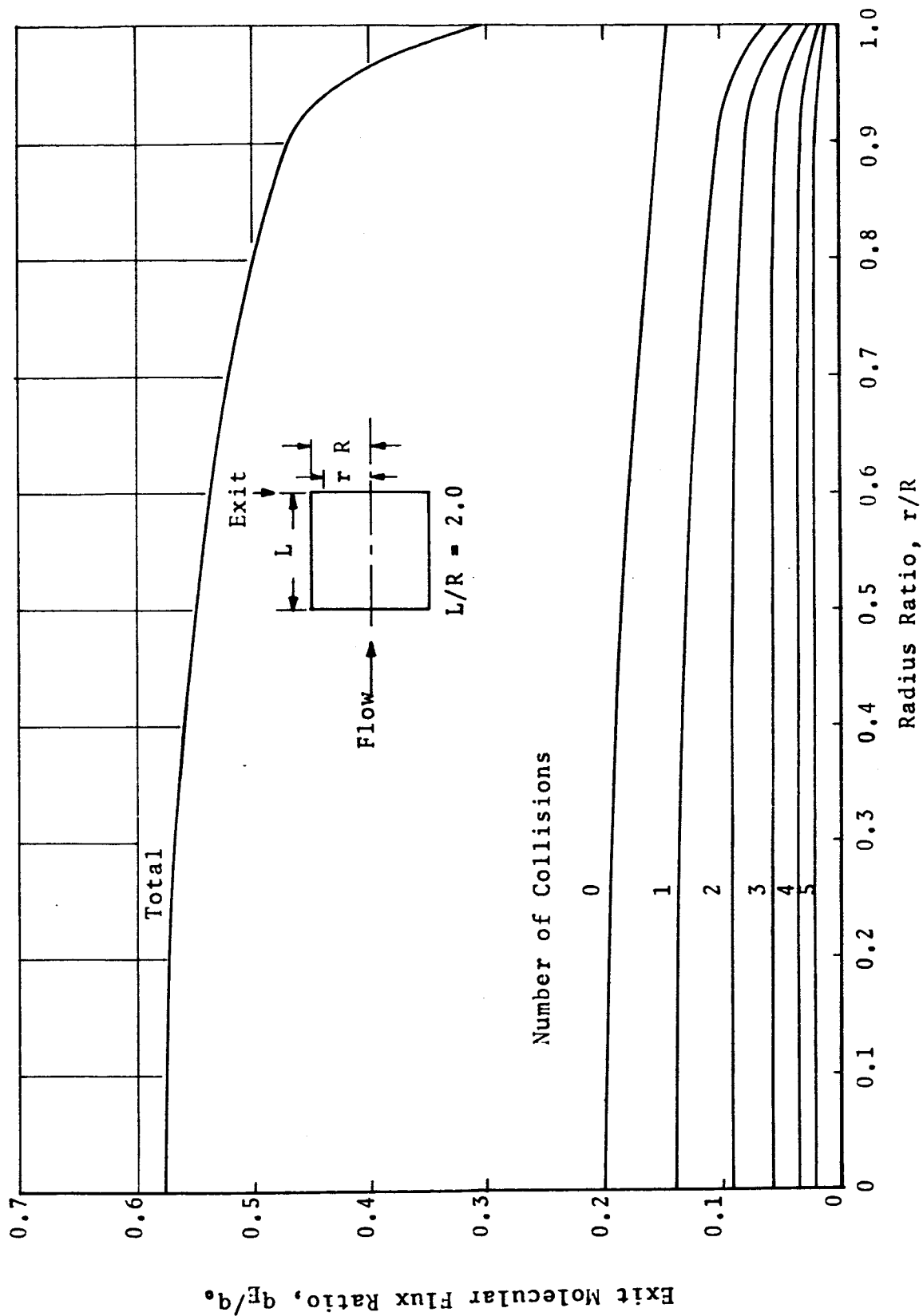FIGURE 2. CENTER EXIT MOLECULAR FLUX AS A FUNCTION OF NUMBER OF COLLISIONS

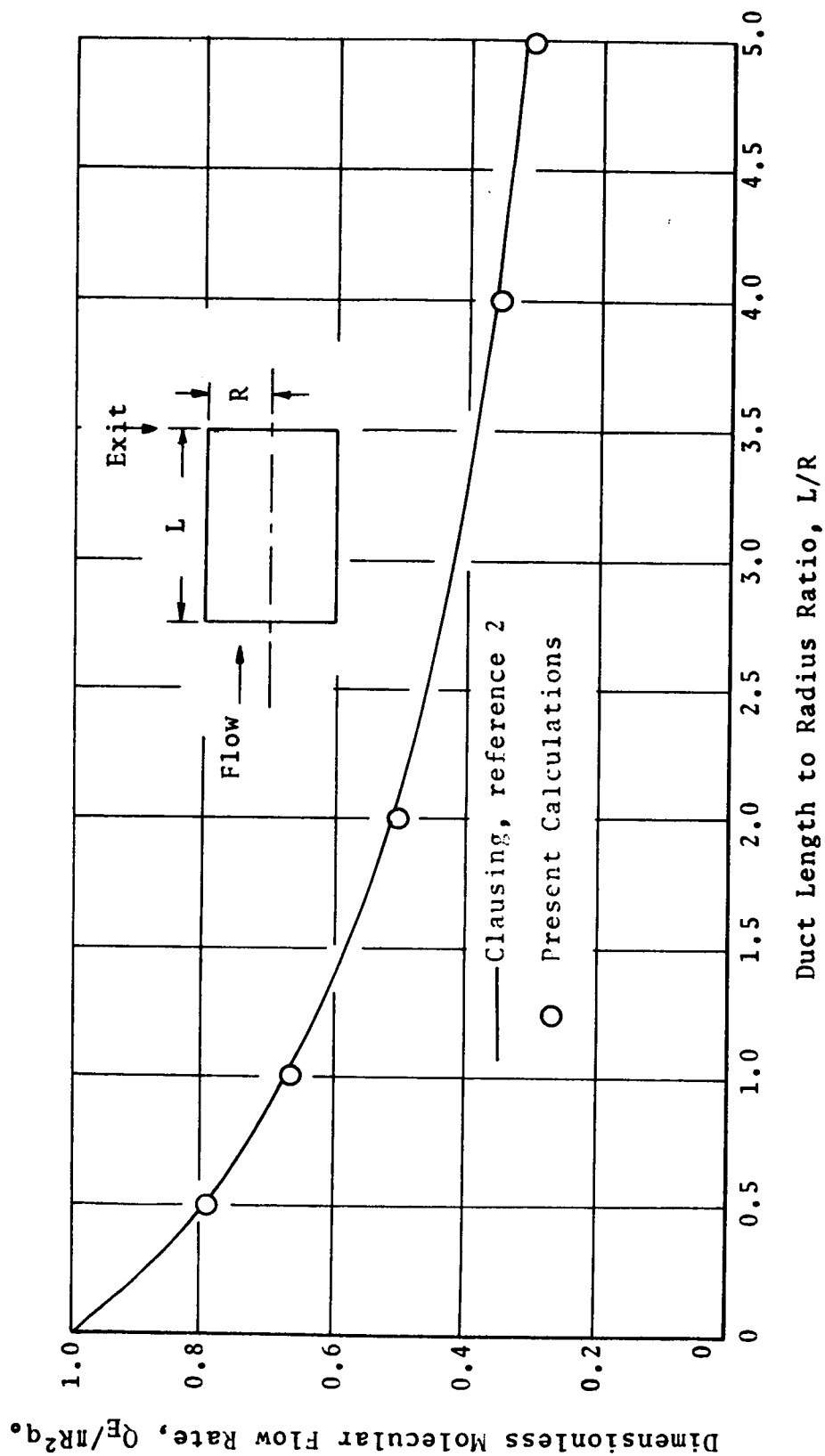FIGURE 3. EXIT MOLECULAR FLUX AS A FUNCTION OF NUMBER OF COLLISIONS AND POSITION

33

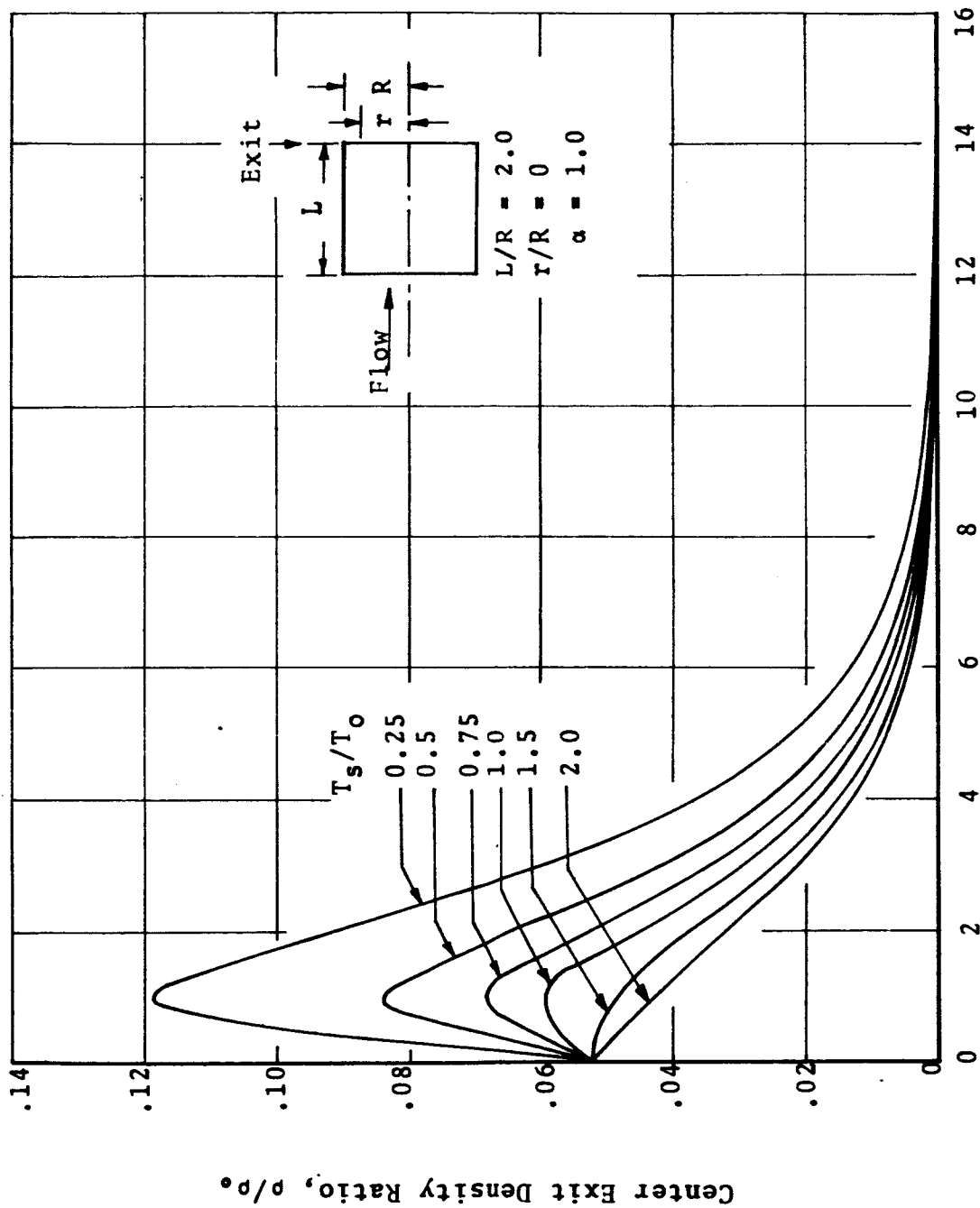FIGURE 4. MOLECULAR FLOW RATE THROUGH DUCT AS A FUNCTION OF DUCT LENGTH TO RADIUS RATIO, L/R

FIGURE 5. CENTER EXIT VOLUME DENSITY AS A FUNCTION OF
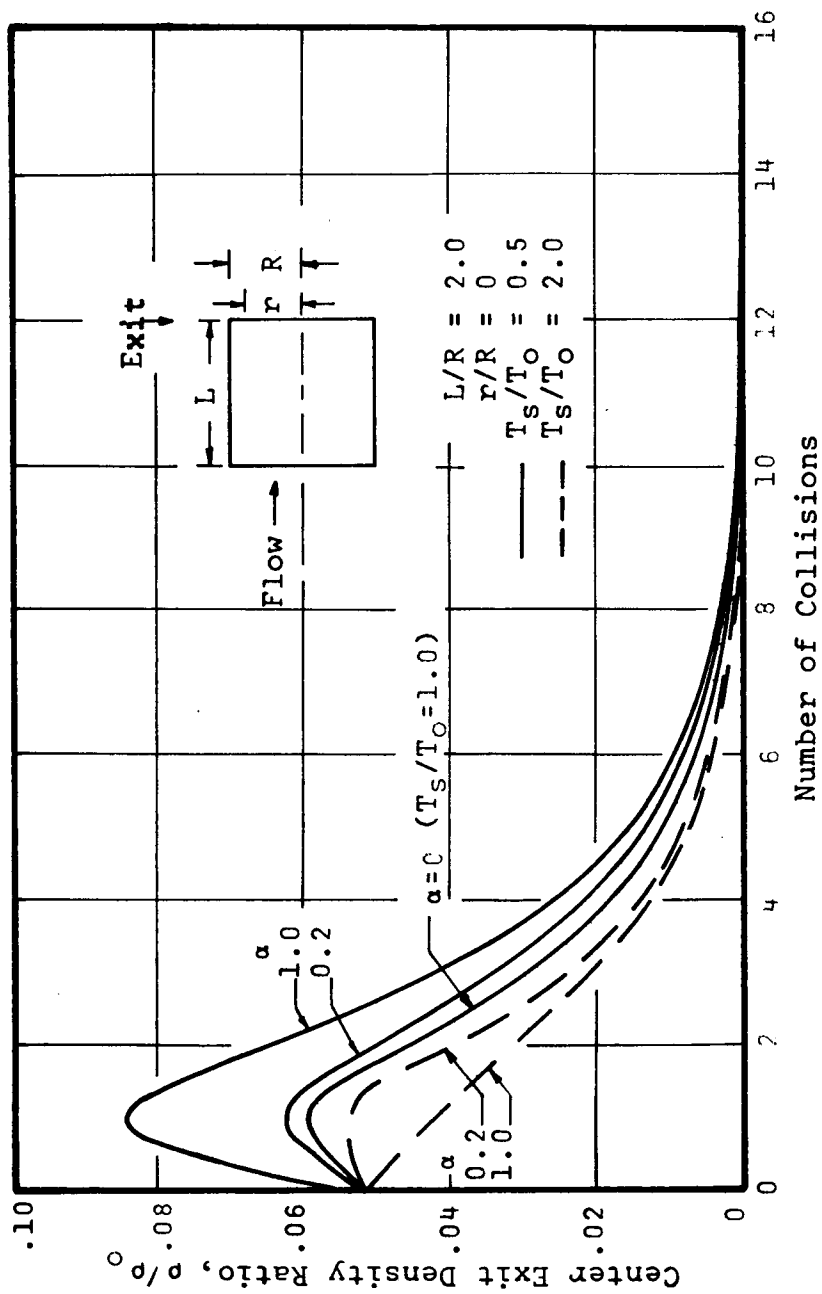NUMBER OF COLLISIONS AND DUCT TEMPERATURE

35

FIGURE 6. CENTER EXIT VOLUME DENSITY AS A FUNCTION OF NUMBER OF COLLISIONS AND THERMAL ACCOMMODATION
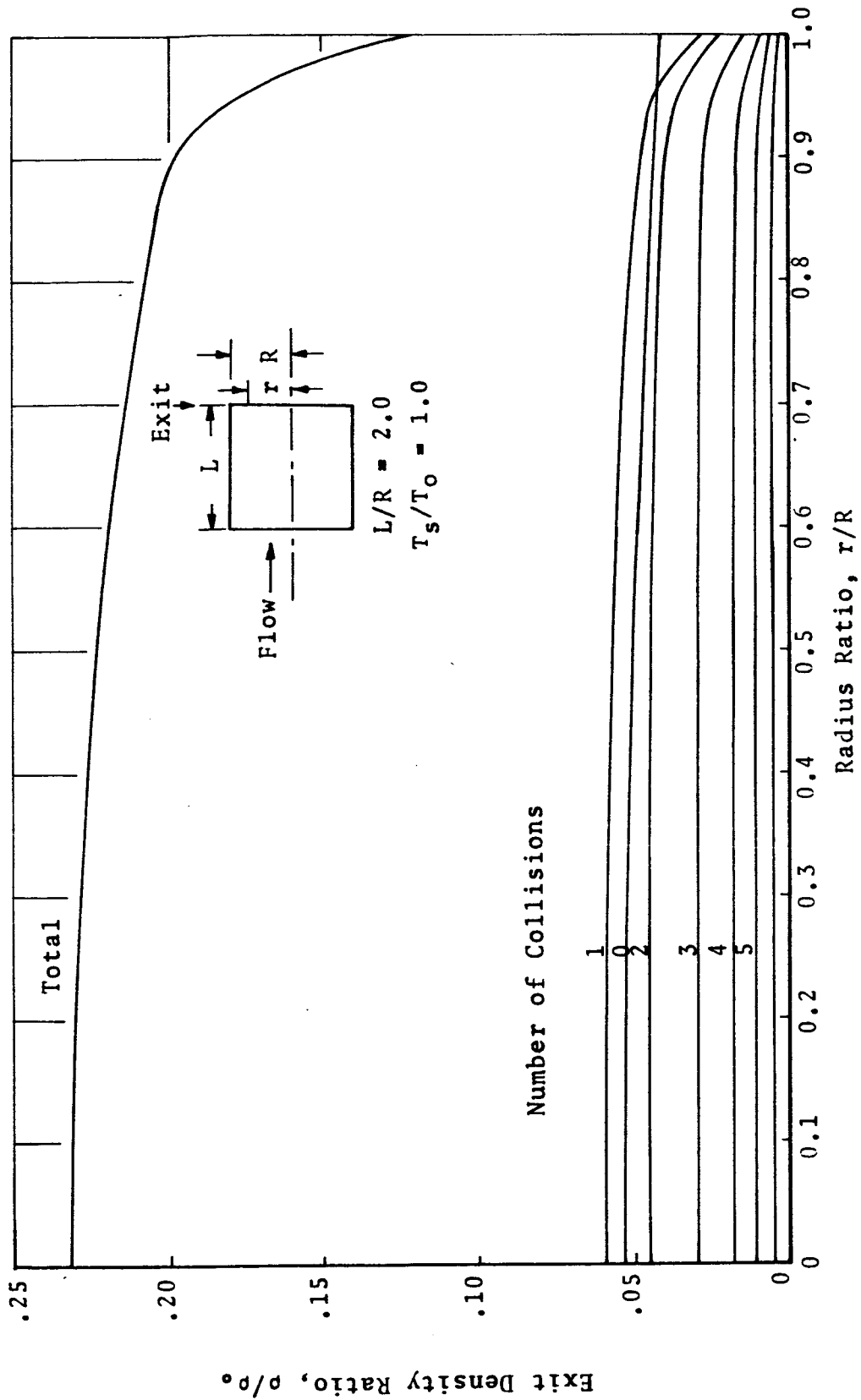
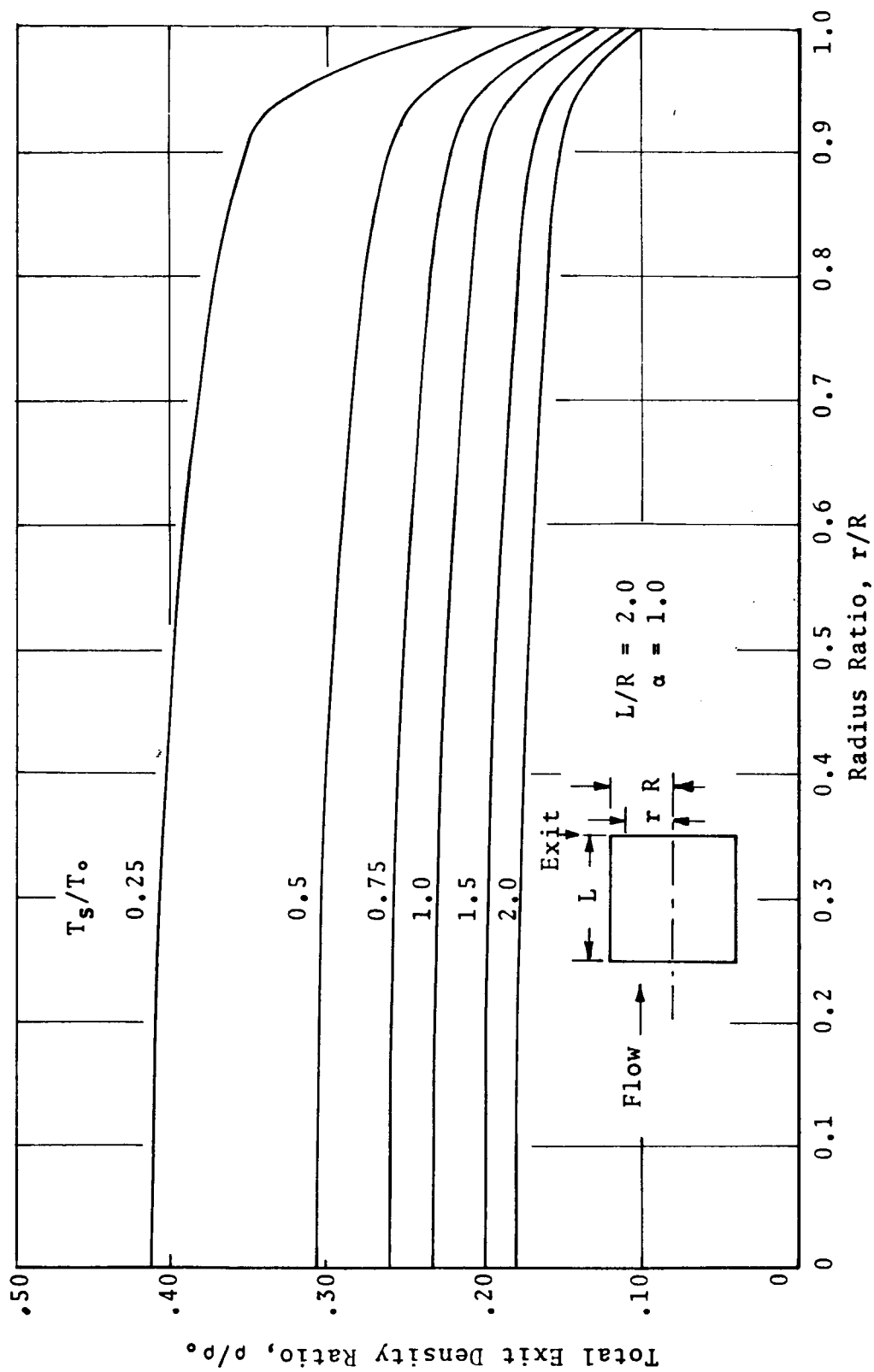FIGURE 7. EXIT VOLUME DENSITY AS A FUNCTION OF NUMBER OF COLLISIONS AND POSITION

FIGURE 8. TOTAL EXIT DENSITY AS A FUNCTION OF
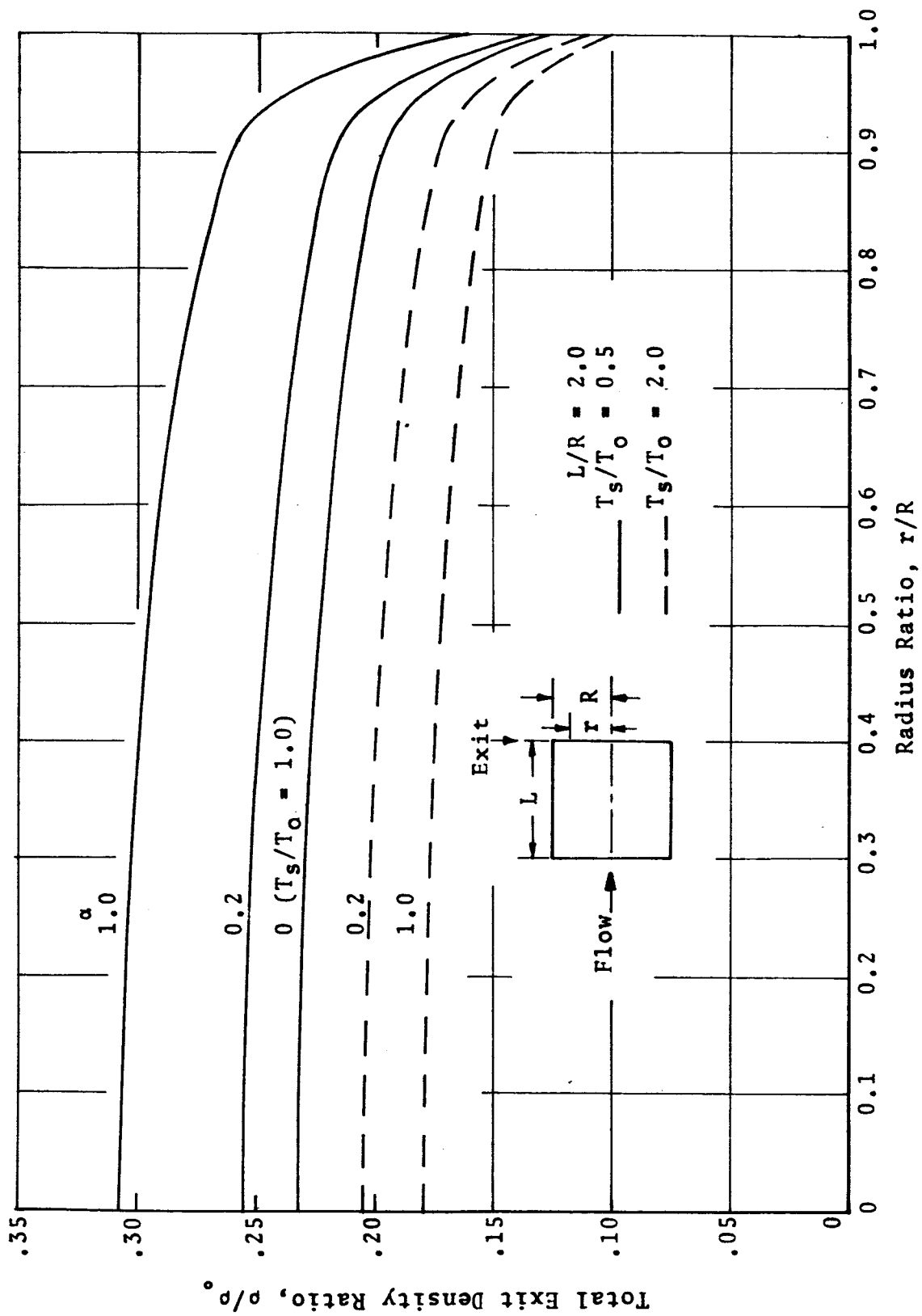DUCT TEMPERATURE AND POSITION

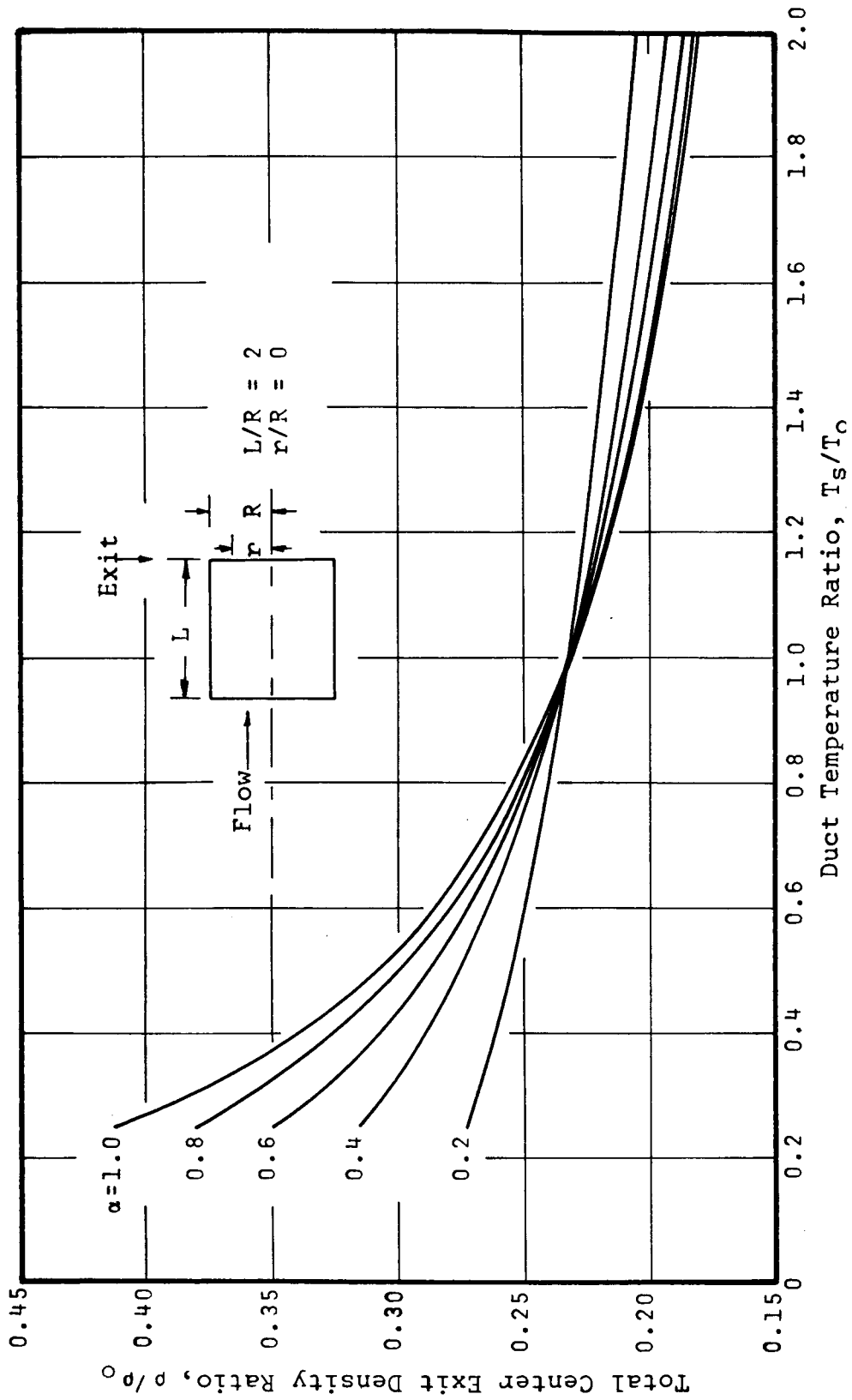FIGURE 9. VARIATION OF EXIT DENSITY DISTRIBUTION WITH THERMAL ACCOMMODATION COEFFICIENT

39

FIGURE 10. VARIATION OF CENTER EXIT DENSITY WITH DUCT TEMPERATURE AND THERMAL ACCOMMODATION COEFFICIENT
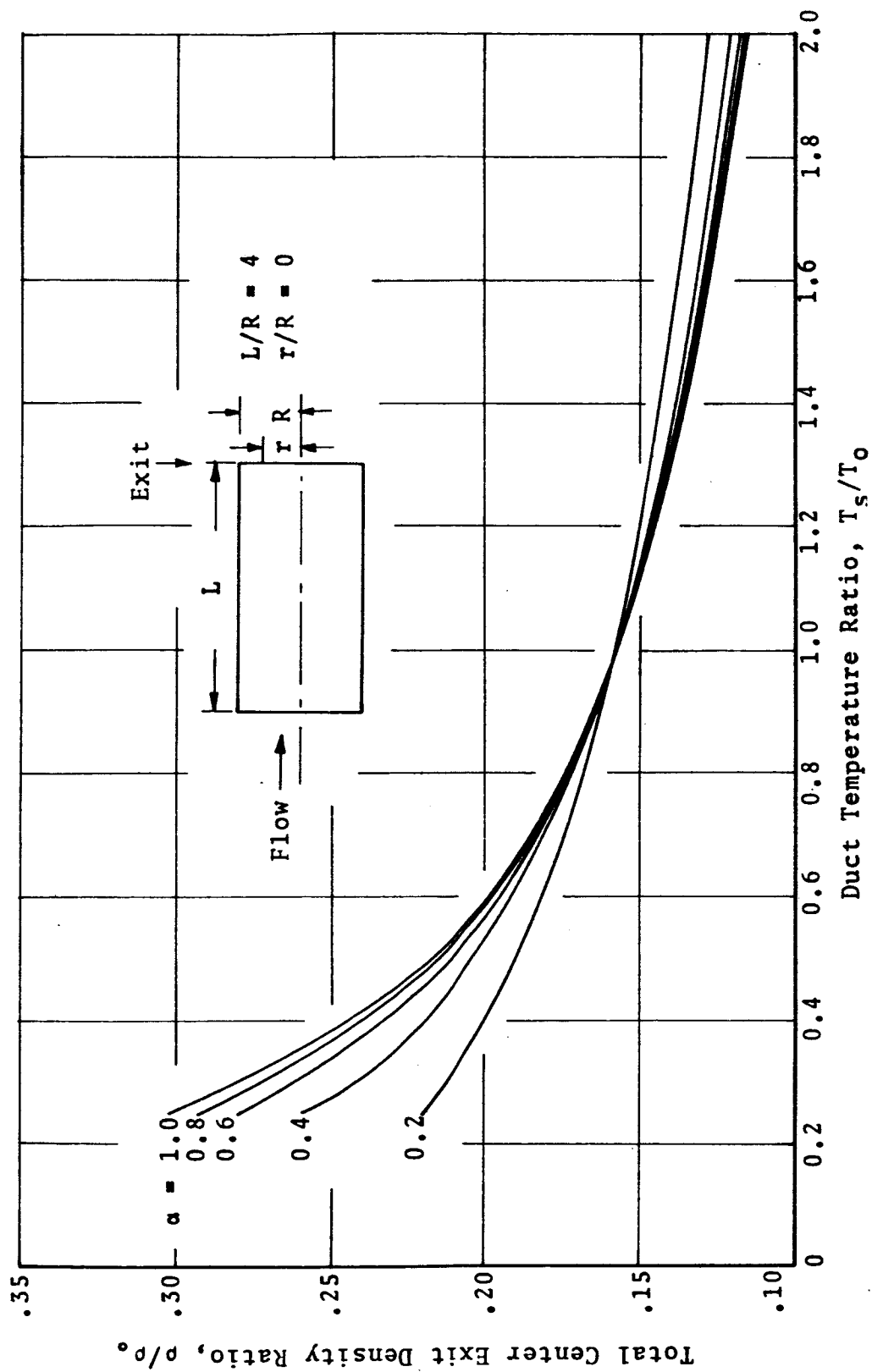
40

FIGURE 11. VARIATION OF CENTER EXIT DENSITY WITH DUCT TEMPERATURE AND THERMAL ACCOMMODATION COEFFICIENT
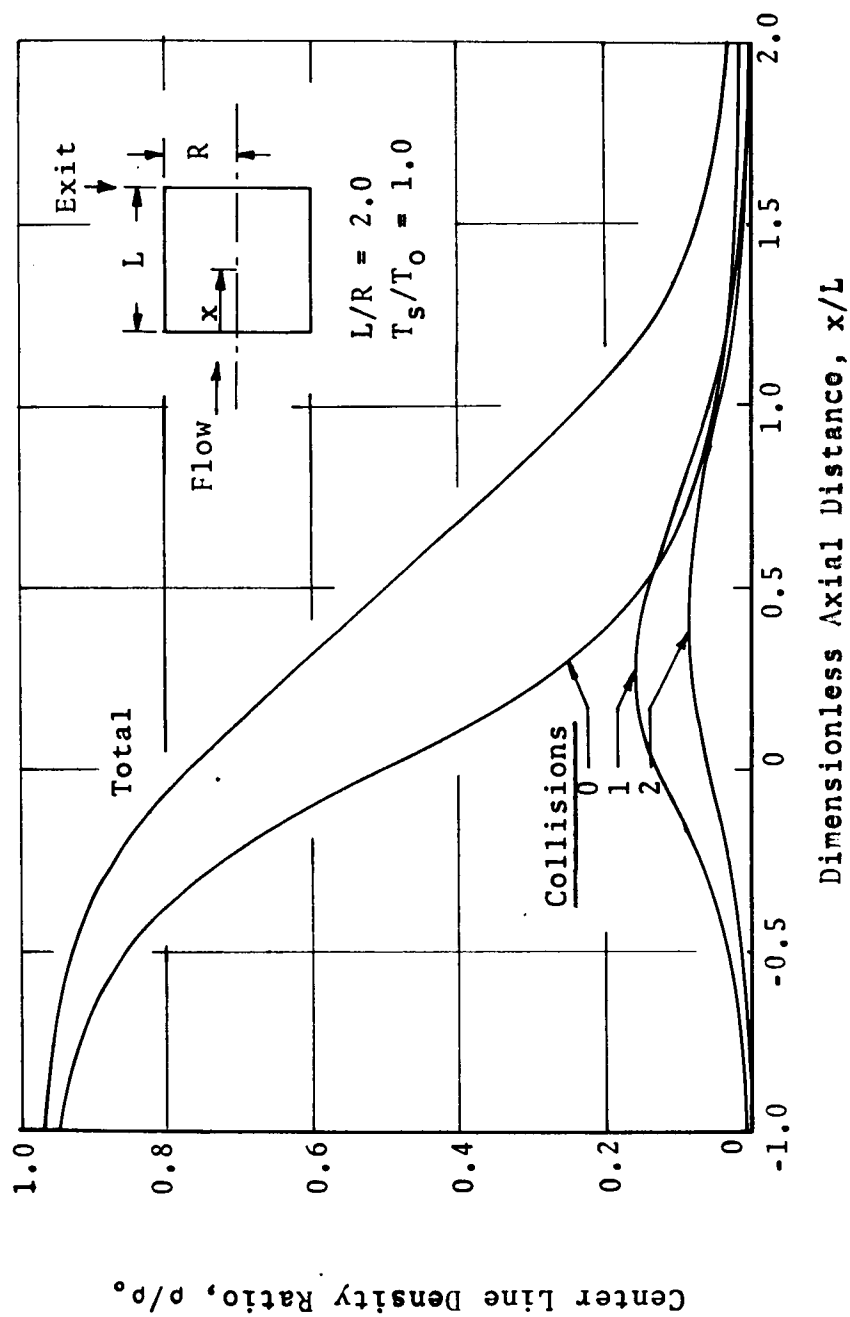
41

FIGURE 12. VARIATION OF CENTER LINE DENSITY DISTRIBUTION
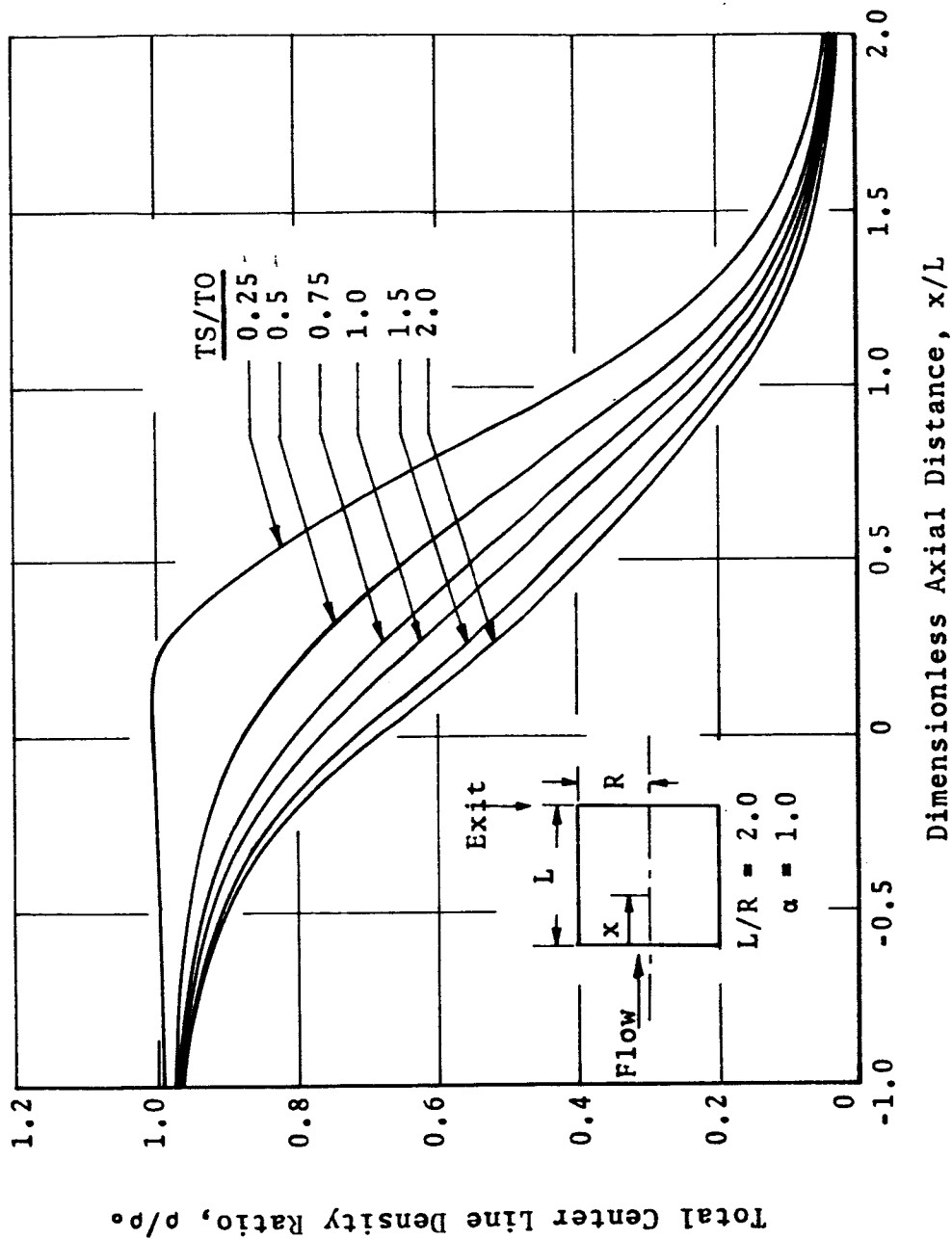WITH NUMBER OF COLLISIONS

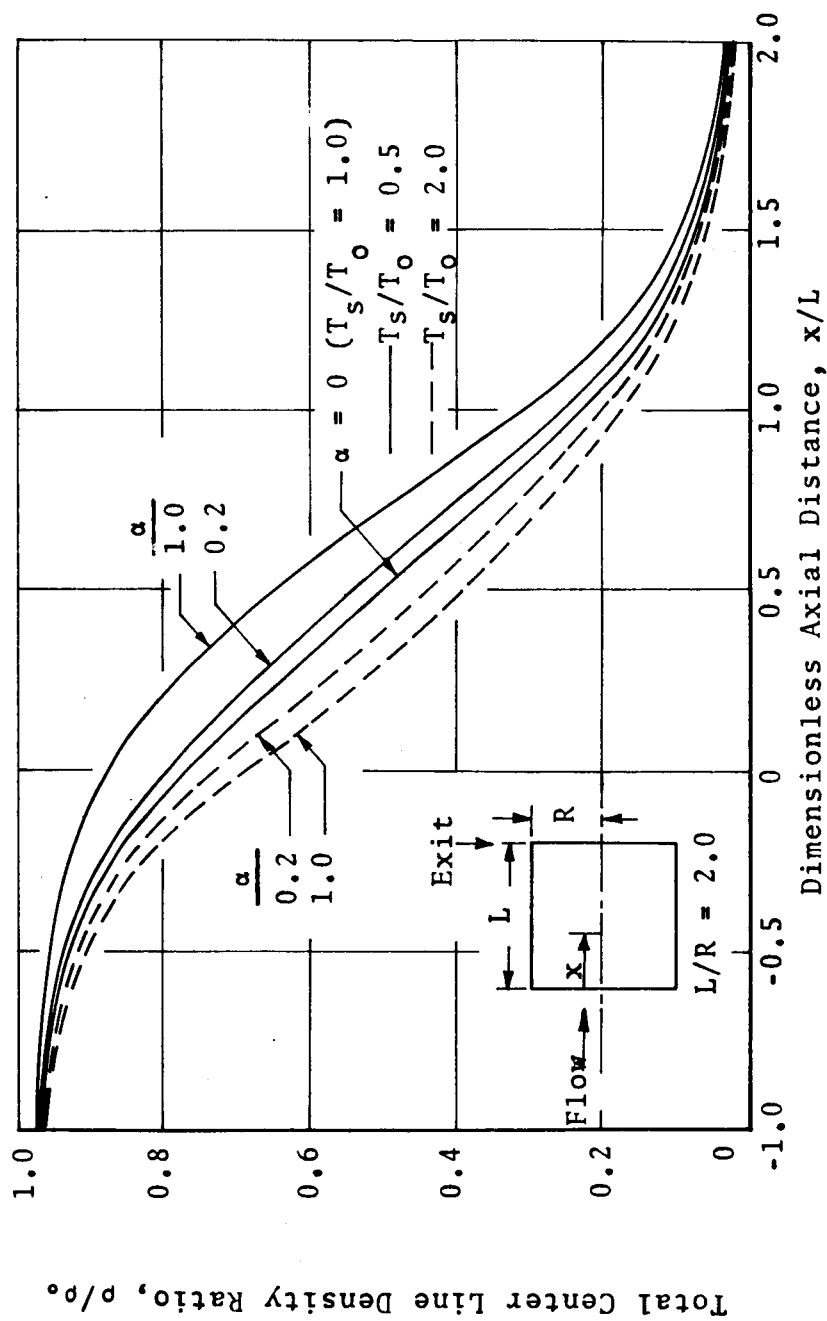FIGURE 13. VARIATION OF CENTER LINE DENSITY DISTRIBUTION WITH DUCT TEMPERATURE

43

FIGURE 14. VARIATION OF CENTER DENSITY DISTRIBUTION WITH THERMAL ACCOMMODATION COEFFICIENT

44

REFERENCES

1. Knudsen, M., _Ann Physik_, 28, 75, 999 (1909); 35, 389 (1911).

2. Clausing, P., _Ann Physik_, 12, 961 (1932).

3. Hottel, H. C. and J. D. Keller, Trans, ASME, IS-55-6, 39 (1933).

4. Demarcus, W. E. and E. H. Hopper, _J. Chem. Phys._, 23, 1344 (1955).

5. Pollard, W. G., and R. D. Present, _Phys. Rev. 73_, 762 (1963).

6. Lozgachev, V. I., _Soviet Physics-Technical Physics 7_, 745, 827 (1963).

7. German, O., _Soviet Physics-Technical Physics_, 7, 834 (1963).

8. Carlson, K. D., P. W. Gillis, and R. J. Thorn, _J. Chem. Phys._, 38, 2064 (1963).

9. Ivanov, B. S., Troitskii, V. S., _Soviet Physics-Technical Physics_, 8, 365 (1963).

10. Troitskii, V. S., _Soviet Physics-Technical Physics_, 7, 353 (1962).

11. Demarcus, W. C., "Oak Ridge Gaseous Diffusion Plant Rept.," K-1302, Parts I-VI (1956-7).

12. Bird, G, A., _Rarefied Gas Dynamics_, edited by L. Talbot (Pergamon Press, Inc., New York, 1960) pp. 245-60.

13. Touryan, K. J., _AIAA Jour._, 2, 559 (1964).

14. Howard, W. M., _Phys. Fluids_, 4, 521 (1961).

15. Gustafson, W. A. and R. E. Kiel, _Phys. Fluids_, 7, 472 (1964).

16. Sparrow, E. M., and A. Haji-Sheikh, _Phys. Fluids 7_, 1256 (1964).

17. Knudsen, M., _The Kinetic Theory of Gases_, John Wiley & Sons, Inc., New York, 1950.

18. Ballance, J. O., W. K. Roberts, and D. W. Tarbell, "A Study of Cryo-pump Configurations in Free-Molecular Flow Regions," _Advances in Cryogenic Engineering_, Vol. 8, p. 57, Plenum Press, New York, 1963.

REFERENCES (Continued)

19. Davis, D. H., _J. Appl. Phys._, 31, 1169 (1960).

20. Link, C. H., "Molecular Kinetics Studies," AEDC-TDR-63-120, Arnold Engineering Development Center, Tenn., 1963.

21. Kennard, E. H., _Kinetic Theory of Gases_, McGraw Hill Book Company, New York, 1938, Chapt. 3.

22. Hamilton, D. C., and W. R. Morgan, "Radiant-Interchange Configuration Factors," NACA TN 2836, National Advisory Committee for Aeronautics, 1952.

23. Hurlbut, F. C., _J. Appl. Phys._, 30, 273-9 (1959).

24. Marton, L., D. C. Schubert, and S. R. Mielczarek, "Electron Optical Studies of Low-Pressure Gases," National Bureau of Standards Monograph 66 (1963).

25. Shephard, J. E. and J. B. Dick, "A Technique for Measuring a Local Gas Density Using Scattered Gamma Radiation," AEDC-TDR 63-87, Arnold Engineering Development Center, Tenn., 1963.

26. Hartnett, J. P., _Rarefied Gas Dynamics_, Edited by L. Talbot (Pergamon Press, Inc., New York, 1960) p. 1.

27. Richley, E. A. and T. W. Reynolds, "Numerical Solutions of Free Molecule Flow in Converging and Diverging Tables and Slots," NASA TN D-2330, June 1964.
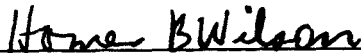
November 2, 1964   APPROVAL   TM X-53156

A STUDY OF DENSITY VARIATIONS IN FREE MOLECULAR FLOW
THROUGH CYLINDRICAL DUCTS DUE TO ACCOMMODATION COEFFICIENTS

By S. J. Robertson

The information in this report has been reviewed for security classification. Review of any information concerning Department of Defense or Atomic Energy Commission programs has been made by the MSFC Security Classification Officer. This report, in its entirety, has been determined to be unclassified.
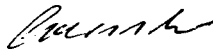
This document has also been reviewed and approved for technical accuracy.

Homer B. Wilson
Chief, Thermoenvironment Branch

Werner K. Dahm
Chief, Aerodynamics Division

E. D. Geissler
Director, Aero-Astrodynamics Laboratory

DISTRIBUTION

DIR

R-DIR

R-ASTR
    Dr. Haeussermann

R-P&VE
    Dr. Lucas
    Mr. Riehl
    Dr. Gayle

R-RP
    Dr. Stuhlinger
    Mr. Heller
    Dr. Shelton
    Mr. Jones
    Mr. Duncan

MS-IP

MS-IPL (8)

MS-T
    Roy Bland

MS-H

HME-P

CC-P

R-AERO
    Dr. Geissler
    Mr. Vaughan
    Mr. Scoggins
    Mr. Dahm
    Dr. Speer
    Mr. Horn
    Mr. Ballance (20)
    Mr. Carter

EXTERNAL DISTRIBUTION

Scientific and Technical Information Facility (25)
Attn: NASA Representative (S-AK/RKT)
P. O. Box 5700
Bethesda, Md.

Langley Research Center
Langley Station
Hampton, Virginia

Oak Ridge National Laboratory
Oak Ridge, Tenn.

University of Minnesota
Minneapolis, Minn.

Dr. Robert Young
University of Tennessee Research Institute
AEDC
Tullahoma, Tenn.

Mason Charok
Code RV-1
NASA Headquarters
Washington D. C.

Lewis Research Center
21000 Brookpark
Cleveland, Ohio
Attn: Dr. Herman Mark
       Mr. Lloyd Krause
       Mr. Edward Richley
       Library

Goddard Space Flight Center
Greenbelt, Md.
Attn: Mr. George Newton
       Library

JPL
4800 Oak Grove Dr.
Pasadena, Calif.

Ames Research Center
Moffett Field, Calif.

Manned Spacecraft Center
Houston, Texas
Attn: William K. Roberts
       Library

Arthur D. Little, Inc.
Cambridge, Mass.
Attn: Raymond Moore

Northrop Space Laboratories
Huntsville, Ala.
Attn: T. M. McCoy

AEDC
Arnold Air Force Station, Tenn.
Attn: Lt. Col. John Peters
       Capt. George Mushalko

ARO, Inc.
AEDC
Arnold Air Force Station, Tenn.
Attn: Mr. George Kirby
       E. K. Latvola
       Library

University of Illinois
Urbana, Ill.

Dr. Robert Stickney
Rm. 3-350
MIT
Cambridge, Mass.

Celestrial Research Corporation
1015 Fremont Avenue
South Pasadena, Calif.
Attn: Dr. Raymond Chuan
       Mr. John Wainwright
       Mr. Don Wallace

University of Alabama
University, Alabama
Attn: Dr. Walter Schaetzle

Institute of Aerophysics
University of Toronto
Toronto, Canada

Cornell Aeronautical Lab., Inc.
Buffalo, New York

McDonnell Aircraft Corp.
P. O. Box 516
St. Louis, Missouri
Attn: E. S. J. Wang

University of Calif. Radiation Lab.
Livermore, Calif.

Lockheed Aircraft Corp.
Huntsville, Ala.
Attn: Mr. M. Culp
       Mr. T. Cunningham
       Mr. L. Morrison
       Library

Brown Engineering Co.
Huntsville, Ala.
Attn: Mr. D. Tarbell
       Library

Heat Technology Laboratory
Huntsville, Ala.
S. J. Robertson (20)

University of Michigan
Ann Arbor, Michigan
Attn: Dr. A. G. Hansen
       Library

Dr. A. B. Huang
Georgia Institute of Technology
Atlanta, Ga.